HOSTED BY

ELSEVIER

CrossMark

Available online at www.sciencedirect.com

ScienceDirect

Progress in Natural Science: Materials International 25 (2015) 251–257

Progress in Natural Science Materials International

www.elsevier.com/locate/pnsmi
www.sciencedirect.com

Original Research

Characteristic analysis on the physical properties of nanostructured Mg-doped CdO thin films—Doping concentration effect

K. Usharani, A.R. Balu*, V.S. Nagarethinam, M. Suganya

PG and Research Department of Physics, A.V.V.M Sri Pushpam College, Poondi 613503, Tamilnadu, India

Received 22 January 2015; accepted 1 May 2015
Available online 8 July 2015

Abstract

Highly conductive and transparent magnesium-doped cadmium oxide (CdO:Mg) thin films have been deposited on suitably cleaned glass substrates maintained at 375 °C by spray pyrolysis technique using perfume atomizer. The magnesium content in the films is varied from 0 to 8 at% in steps of 2 at%. The effect of Mg doping on the structural, morphological, optical and electrical properties of the CdO thin films has been studied. All the films exhibited cubic structure with a preferential orientation along the (1 1 1) plane irrespective of the Mg doping level. SEM analysis showed that the film morphology modifies from spherical shaped grains to closely packed cauliflower shaped nanostructures with Mg doping. Except for the film coated with 2 at% Mg dopant, all the other doped films exhibited a blue shift in the optical band gap. Electrical studies revealed that the CdO:Mg film coated with 8 at% Mg dopant had a minimum resistivity of 0.0853×10^{1} Ω-cm.

Keywords: X-ray diffraction; Texture coefficient; Thin films; Optical band gap; Electrical properties

1. Introduction

Thin film materials exhibiting high electrical conductivity and optical transparency are used extensively in a variety of applications including architectural windows, thin film photovoltaic and many other opto-electronic devices [1,2]. Transparent conducting oxide (TCO) thin films have great importance as transparent electrodes in flat-panel displays, solar cells and among these TCOs, cadmium oxide (CdO) is technologically important due to its high transparency in the visible range of the electromagnetic spectrum and high electrical conductivity due to moderate electron mobility and high carrier concentration [3]. CdO is an n-type semiconductor with a band gap of ~2.5 eV [4]. The features of high conductivity, high transparency and low band gap make it suitable for various applications such as photodiodes [5], phototransistors [6], transparent electrodes, liquid crystal displays [6], IR detectors and anti-reflection coatings [7]. Due to its low optical band gap, CdO is not widely used in optoelectronics and photovoltaic applications. It is reported that the optical properties and thus the optical band gap of CdO can be modified by doping with aluminium [8]. Deokate et al. [9] have reported that fluorine doping increases the band gap of CdO films. Tin doping produces a blue shift in the optical band gap and a decrease in the electrical conductivity of CdO films [10]. Benhaliliba et al. [11] have reported a blue shift in the optical band gap of Cu-doped CdO thin films. Band gap widening was also observed in Zn-incorporated CdO thin films [12]. Pan et al. [13] have reported that the optical band gap of CdO films deposited by rf magnetron sputtering increases with gadolinium (Gd) doping. Yakuphanoglu [14] reported that the optical band gap of the CdO film can be engineered over a wide range of 2.27–2.45 eV by introducing boron dopant. Flores-Mendoza et al. [15] observed an increase in the optical band gap of CdO thin films with In doping. These results infer that the optical and electrical properties of CdO can be enhanced by doping with suitable transition elements. Magnesium is a transition metal which may modulate the value of band gap of CdO and increase its UV luminescence intensity. Magnesium belongs to *P*63/*mmc* space group similar to that of cadmium. Mg^{2+} has an ionic radius of 0.72 Å, which is less than that of Cd^{2+} (0.97 Å). The electronegativity of Mg is 1.31

*Corresponding author. Tel.: +91 9442846351.
E-mail address: arbalu757@gmail.com (A.R. Balu).
Peer review under responsibility of Chinese Materials Research Society.

http://dx.doi.org/10.1016/j.pnsc.2015.06.003

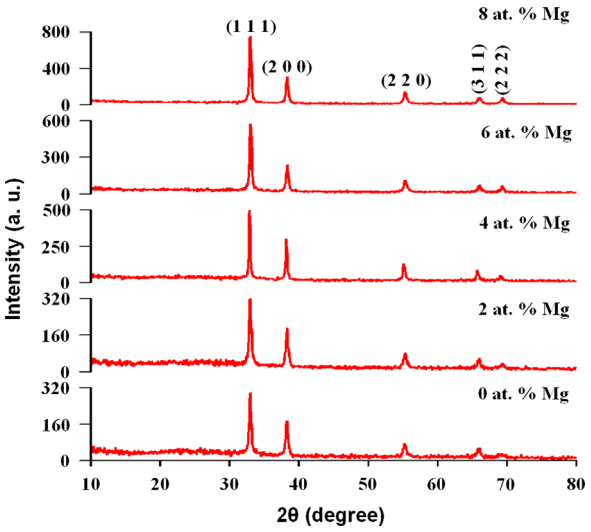

Fig. 1. XRD patterns of CdO:Mg thin films with different Mg doping concentrations.

Pauling which is slightly lower than that of cadmium (1.69 Pauling). So it can be expected that Mg^{2+} ions substituting Cd^{2+} ions in the CdO lattice should improve its electrical and optical properties. Recently Gupta et al. [16] has studied the effect of growth parameters on Mg-doped CdO films grown by pulsed laser deposition (PLD). Besides this, the studies on spray deposited Mg-doped CdO films are scarce in the literature. So in this work, spray pyrolysis technique using perfume atomizer is used to deposit Mg-doped CdO thin films with different Mg concentrations (0, 2, 4, 6 and 8 at%) and investigations on the structural, morphological, optical and electrical properties of the CdO films due to Mg doping is made. To the best of our knowledge, there is no previous report on the properties of Mg-doped CdO (CdO:Mg) films deposited by spray pyrolysis technique using perfume atomizer.

2. Experimental details

Mg-doped CdO thin films were deposited on the glass substrates by employing a simplified and low cost spray pyrolysis technique. The spray pyrolysis apparatus used in this work consists of a perfume atomizer, a substrate holder with heater and an enclosure. In the preparation of CdO thin films, 0.1 M cadmium acetate was used as the precursor salt and double distilled water was used as the solvent. To achieve Mg doping, magnesium acetate with different concentrations (0, 2, 4, 6 and 8 at%) was mixed with the starting solution. All the salts used were of analytical reagent grade (Sigma make) with a purity of 99.9%. Microscopic glass slides with dimensions 75 × 25 × 1.2 mm^3 were used as substrates. The resultant precursor solution was sprayed on preheated substrates kept at 375 °C using a chromel–alumel thermocouple. The optimized deposition parameters such as substrate-spray nozzle distance (25 cm), spray angle (45°), spray time (5 s), spray interval (10 s) and spray rate (6 ml/min) were kept constant during deposition. After deposition, the coated substrates were allowed to cool down to room temperature. The possible chemical reaction involved in the formation of CdO:Mg thin films is as follows:

$$Cd(Mg)(CH_3COO)_2 + 5H_2O \rightarrow \Delta \rightarrow CdMgo\downarrow + 8H_2\uparrow + 4CO_2\uparrow$$

The thickness of the films was estimated using profilometer (SurfTest SJ-301). The thickness of CdO:Mg films coated with 0, 2, 4, 6 and 8 at% Mg concentrations were found to be equal to 531, 565, 536, 544 and 581 nm respectively. X-ray diffraction (XRD) patterns were obtained using X-ray diffractometer (PANalytical PW 340/60 X'pert PRO) which was operated at 40 kV and 40 mA with Cu$K\alpha$ ($\lambda = 1.5406$ Å) radiation. The sample was mounted at 2.5° and scanned from 10 to 80° in steps of 0.02° with a scan rate of 1.2 ° min^{-1}. Scanning electron microscopy (SEM) images and optical transmission spectra were obtained at room temperature using scanning electron microscope (HITACHI-S-300H) and UV–vis–NIR double beam spectrophotometer (Perkin Elmer LAMBDA-35) with unpolarised light at normal incidence in the wavelength range from 300 to 1100 nm respectively. Electrical studies were carried out at room temperature using four point probe apparatus.

3. Results and discussion

3.1. Structural studies

The X-ray diffraction patterns of Mg-doped CdO thin films deposited at 375 °C using perfume atomizer with various Mg concentrations (0, 2, 4, 6 and 8 at%) are shown in Fig. 1. The XRD patterns reveal that all the films are polycrystalline in nature with cubic crystal structure. The diffraction peaks observed at $2\theta = 32.986°$, 38.267°, 55.25°, 65.9° and 69.19° were indexed as (1 1 1), (2 0 0), (2 2 0), (3 1 1) and (2 2 2) planes of pure CdO (JCPDS Card No. 73-2245). The calculated interplanar distance and standard '*d*' values of the films are given in Table 1. The almost matching of the calculated and standard '*d*' values confirm that the deposited films belong to pure CdO. The high diffraction intensity of the peak at $2\theta = 32.9°$ observed for all the films indicates that the films have preferential orientation along the (1 1 1) direction. The preferred growth is always favored by a high substrate temperature and specific interaction of the nucleus with the

Table 1
Comparison of calculated and standard '*d*' values of CdO:Mg thin films.

(*h k l*) Planes	Standard '*d*' (Å)	Calculated '*d*' (Å) Mg doping concentration (at%)				
		0	2	4	6	8
(1 1 1)	2.7129	2.7133	2.7139	2.7134	2.7130	2.7131
(2 0 0)	2.3495	2.3501	2.3487	2.3547	2.3458	2.3479
(2 2 0)	1.6613	1.6612	1.6596	1.6640	1.6589	1.6593
(3 1 1)	1.4168	1.4161	1.4158	1.4191	1.4145	1.4145
(2 2 2)	1.3564	1.3567	1.3559	1.3583	1.3534	1.3545

substrate surface. The surface energy of interaction determines the plane of orientation to be preferred; such as the orientation having low surface energy of interaction is favored. The observed preferential orientation along the (1 1 1) plane here confirms that along this plane the surface energy should be minimum. The preferential orientation along the (1 1 1) plane observed here exactly matches with Usharani et al. [17] for CdO thin films fabricated by spray pyrolysis technique using perfume atomizer. Tokeer Ahmad et al. [18] also reported a similar cubic structure for Mn-doped CdO thin films synthesized by solvothermal method. It has been observed that the preferential orientation of (1 1 1) plane remained predominant for all the films irrespective of Mg doping concentration, indicating that the incorporation of Mg into the Cd sites does not alter the preferential growth. The predominance of the (1 1 1) plane observed here with Mg concentration exactly matches the results observed by Vigneshwaran et al. [19] for Mg-doped CdO films prepared by spray pyrolysis technique. No peaks relating to MgO were observed in the patterns, indicating the purity of the CdO films.

It can be observed from Table 1, that the value of interatomic spacing initially increases with Mg doping up to 2 at% and then it decreases for further doping concentration. The increased value of *d*-spacing observed for the CdO:Mg film with 2 at% Mg infers that magnesium atoms are placed in the grain boundaries or at the film surface with simultaneous penetration into grains [20]. Herewith, the diffusion of Mg into grain proceeds by the dissociative mechanism—the migrating impurity quickly moves by way of interstitial sites and settles in vacancies [21]. The lesser values of *d*-spacings observed above 2 at% Mg doping infers that Mg^{2+} ions replace Cd^{2+} ions in the host lattice substitutionally.

XRD patterns also revealed that the doping of Mg induces a variation of the film growth texture. The texture of a particular plane can be represented by the texture coefficient *TC* (*hkl*), which can be calculated from X-ray data using the formula [22]:

$$TC(hkl) = \frac{I(hkl)/I_o(hkl)}{N^{-1}\sum_N I(hkl)/I_o(hkl)} \quad (1)$$

where *I*(*hkl*) is the measured relative intensity of the plane (*hkl*), I_o(*hkl*) is the standard intensity of the plane (*hkl*) taken from the JCPDS data, and *N* is the number of reflections. Any deviation of the calculated TC value from unity implies preferred growth. The texture coefficient values of CdO:Mg films calculated for the diffraction peak (1 1 1) and (2 0 0) are compiled in Table 2. It can be seen from the table that, the value of TC(1 1 1) initially decreases with Mg doping up to 2 at% and then it increases linearly with increase in Mg content in the films, whereas TC (2 0 0) show an opposite trend behaviour. This is a consequence of re-orientational effect in crystalline structure of CdO. Similar behaviour was reported by Manjula et al. [23] for CdO thin films prepared by spray pyrolysis technique using perfume atomizer. The strengthening of (1 1 1) and weakening of (2 0 0) plane for higher Mg doping concentrations may be attributed to the presence of internal stress induced by the doping of Mg during spray deposition, which can alter the energetic balance between different crystal plane orientation and lead to preferred texture growth. This is in accordance with Zheng et al. [24] for Sn-doped CdO films obtained by pulsed laser deposition.

The average grain size (D) of Mg doped CdO films are calculated using the Scherrer formula [25]:

$$D = \frac{0.94\lambda}{\beta \cos \theta} \quad (2)$$

where λ is the wavelength of the X- ray used (1.5406 Å), β is the full width at half maximum of the strongest peak, and θ is the Bragg angle. The calculated *D* values for the (1 1 1) plane of CdO:Mg films are given in Table 2[1].

It can also be observed from Table 2 that the diffraction angle of (1 1 1) and (2 0 0) planes are slightly shifted towards higher 2θ angle for the films coated with 4, 6 and 8 at% Mg concentrations due to the shrinkage of the lattice parameter values (Table 2). The slight decrease of lattice constant is due to the decrease in interatomic spacing which results by the substitution of smaller Mg^{2+} ions (0.72 Å) into larger Cd^{2+} ions (0.97 Å). The slight increase of lattice constant values observed for the film coated with 2 at% Mg concentrations might be due to Mg^{2+} ions placed in the grain boundaries or at the film surface not successfully replacing Cd^{2+} ions in the host CdO lattice.

3.2. SEM analysis

Fig. 2(a–e) shows the SEM images of CdO:Mg thin films fabricated by the spray technique using perfume atomizer with different Mg doping concentrations (0, 2, 4, 6 and 8 at%). It is apparent from the SEM images that all the films show uniform surface with well-defined grain boundaries. Un-doped CdO film (0 at% Mg) shows spherical grains interconnected with each other. Traces of few empty sites are also evident from the SEM image of the undoped sample (Fig. 2(a)). With increase in Mg doping, the grains starts to modify with traces of cauliflower shaped nano-structures as observed for the film coated with 2 at% dopant (Fig. 2(b)). With further increase in doping concentration, closely packed grains with cauliflower shaped nanostructures starts to bloom throughout the entire surface of CdO:Mg film coated with 4 at% Mg (Fig. 2(c)). Grains with well modified cauliflower shaped structures are evident for the film coated with 6 at% Mg concentration (Fig. 2(d)). As the doping concentration is increased further, surface modifies with closely packed cauliflower shaped nanostructures with different sizes as evident from (Fig. 2(e)) for the CdO:Mg film coated with 8 at% Mg. The film surface appears more compact and dense which is an indication of improved crystallinity of this film which very well acknowledges the results obtained for this film in XRD analysis (Section 3.1). In nano-scale dimension, CdO thin films exhibit numerous structures like nanoparticles [26], nano-wires [27],

[1]It is seen that the average grain size is in the range of 24–30 nm, showing only a slight variation with Mg doping concentration. The relatively small grain size means low surface roughness of the films, which can lead to a decrease in the propagation loss of surface acoustic wave (SAW) devices and an increase in the efficiency for photovoltaic solar cells.

Table 2
Structural parameters and electrical resistivity of CdO:Mg thin films.

Mg doping concentration (at%)	2θ		Texture coefficient, TC		Lattice constant, 'a' (Å)	Average grain size, D (nm)	Strain, $\varepsilon \times 10^{-3}$	Electrical resistivity, $\rho \times 10^{1}$ Ω-cm
	(1 1 1)	(2 0 0)	(1 1 1)	(2 0 0)				
0	32.986	38.267	9.0745	4.9983	4.6995	27.63	1.254	2.002
2	32.904	38.190	9.0090	5.0101	4.7006	29.73	1.422	4.901
4	32.987	38.201	9.1820	4.9264	4.6994	24.38	1.380	3.311
6	33.052	38.341	9.3652	4.7820	4.6991	25.12	1.298	0.664
8	33.006	38.305	9.5336	4.7259	4.6992	26.26	1.256	0.0853

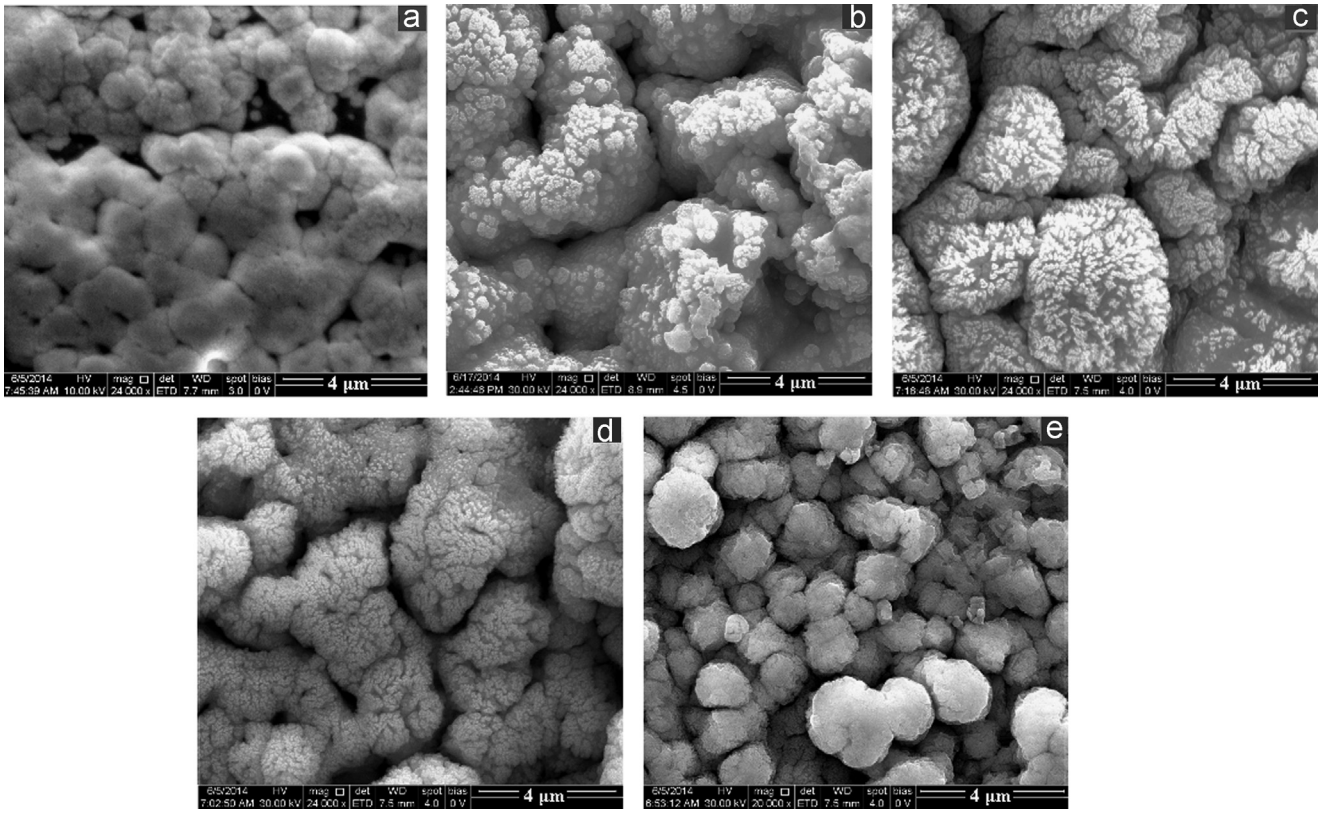

Fig. 2. SEM images of Mg-doped CdO thin films coated with different Mg concentrations.

nano-needles [28], and nano-crystals [29]. Among these structures of this compound, cauliflower like structure emerges from the construction of nanorods bundles. The SEM images of the CdO:Mg thin films coated here showed cauliflower like structures which might have been formed from interwovened nanorods. Similar structures were reported by Usharani et al. [12] for spray deposited Zn-doped CdO films. Tadjarodi et al. [30] reported that CdO with cauliflower like structure showed high performance on the removal of Congo red from aqueous solution due to its high adsorption capacity.

3.3. Elemental analysis

In order to confirm the presence of the dopant, CdO:Mg films were subjected to EDS analysis. The EDS spectra shown in Fig. 3 confirm the presence of Mg in the doped films. The atomic percentage compositions of the elements were shown in the insets. It is seen that the amount of Mg increases with increase of the doping concentration. It is also noted that above 2 at% Mg concentration, Cd content decreases as the doping concentration increases which very well support the substitution of Cd^{2+} ions with Mg^{2+} ions in the host lattice.

3.4. Optical characterization

Fig. 4 depicts the transmittance spectra of undoped CdO and Mg-doped CdO films within the wavelength range 300–1100 nm. It is observed that except for the CdO film coated with 2 at% Mg, the transparency increases to a large extent. The maximum transmittance of the CdO:Mg film coated with 8 at% Mg is nearly equal to 90% for wavelengths over 500 nm. The high transmittance for the doped films is an indication that the films are highly

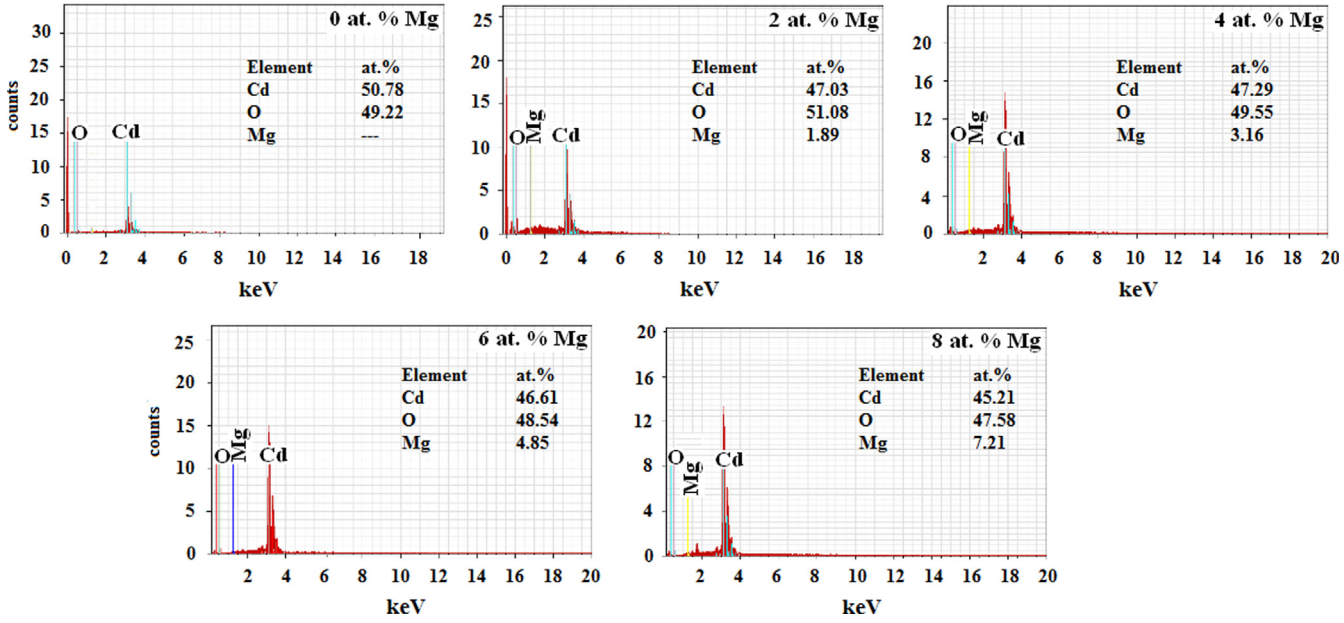

Fig. 3. EDAX spectra of Mg-doped CdO thin films.

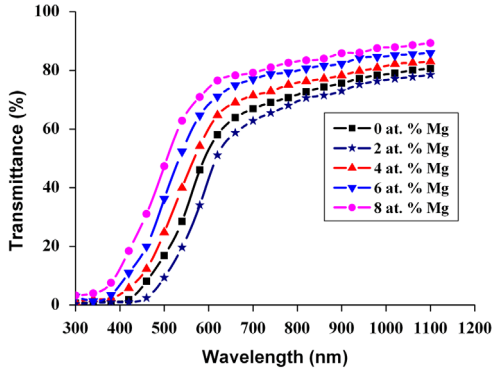

Fig. 4. Transmittance spectra of Mg-doped CdO thin films.

crystalline and with high degree of stoichiometry. Due to extremely good transmittance in the visible as well as in IR regions, CdO:Mg films are considered as very good window material in solar cell applications. The low transparency observed for the film coated with 2 at% Mg doping might be due to increased thickness (565 nm) observed for this film as evident from Section 2. Increased film thickness results in increased absorption by free carriers [31] which might be due the increased crystallite size value obtained for this film. Expect for the CdO:Mg film coated with 2 at % Mg dopant, the optical transmittance spectra of CdO:Mg films show the shifting of the band edge towards low energy suggesting that their band gaps should increase. The values of band gap were calculated using the fundamental absorption, which corresponds to electron excitation from the valance band to conduction band [32]. The absorption coefficient (α) and the incident photon energy ($h\nu$) are related by the relation [33]:

$$(ahv)^{1/n} = A(hv - E_g) \quad (3)$$

where A is constant, E_g is the band gap. The band gap values can be estimated by extrapolating the linear part of the plot of $(\alpha h\nu)^2$ versus $h\nu$ to $\alpha = 0$ as shown in Fig. 5. The band gap of pure CdO film (0 at% Mg) is found to be equal to 2.38 eV. This value exactly matches with the value obtained by Ma et al. [34] for sputtered CdO thin film. The band gap values of CdO:Mg films with 2, 4, 6 and 8 at% Mg concentrations were found to be equal to 2.3, 2.41, 2.45, and 2.5 eV respectively. Expect for the film coated with 2 at% Mg doping, the band gap value increases for all the doped samples, i.e. they exhibit a blue shift with increasing Mg concentration. Generally, blue shift observed in doped CdO thin films, can be related to Burstein–Moss (BM) effect. Wang et al. [35] have observed an enhancement of band gap in Co-doped ZnO thin films. Normally the dopant elements always leads to an increase or decrease of electrons in the conduction band which shifts the Fermi level with a simultaneous change in the band gap energy. The increase in the band gap values of CdO thin films coated with 4, 6 and 8 at% Mg doping is due to increase in free electron concentration which indicates that most of the Mg^{2+} ions substitutes uniformly for Cd^{2+} in the host lattice. Quantum confinement also provides an alternative and fundamental explanation for the band gap variation of doped films [36].

It is well known that when a semiconducting film is undoped, the Fermi level of the bulk (E_f(bulk)) is located at the midgap between the conduction band and the valence band and is equal in energy to the surface Fermi level (E_f (surf)). There is no charge transfer between the bulk and the surface, so the bands are flat. If the film is n-type doped, E_f(bulk) is closer to the conduction band, which is higher than E_f(surf) under disequilibrium. The electrons will transfer from the bulk to the surface. E_f(bulk) drops and E_f(surf) rises until equilibrium is achieved. At equilibrium, the energy bands bend upward as one move towards the surface. In nanocrystalline materials, band bending effect takes place only when dopant ions or partially charged interstitial ions move into the host

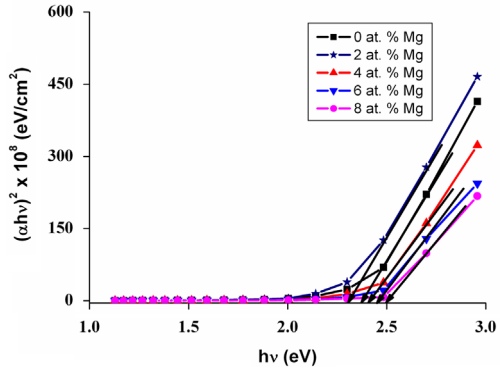

Fig. 5. Plots of $(\alpha h\gamma)^2$ versus $h\gamma$ of Mg-doped CdO films.

lattice. Usually the band bending effect decreases with the size of the crystallites of semiconductor particle. The smaller crystallite size values obtained for the CdO:Mg films coated with 4, 6 and 8 at% Mg concentrations (Table 2) results in the decrement of the band bending effect which enhances their optical band gap values.

3.5. Electrical studies

The electrical resistivity values of CdO:Mg thin films is presented in Table 2. It can be seen that all the films have a resistivity in the order of 10^1 Ω-cm. Undoped sample have a resistivity of 2.002×10^1 Ω-cm which exactly matches with the value obtained by Shanmugavel et al. [37] for the CdO film coated by spray pyrolysis technique using perfume atomizer. The resistivity value increases with Mg doping concentration and attains a maximum value (4.901×10^1 Ω-cm) for the film coated with 2 at% Mg. With further increase in Mg concentration, it decreases and attains a minimum value of 0.0853×10^1 Ω-cm for the film coated with 8 at%. This agrees with d(1 1 1) values variation with Mg doping. The high value of resistivity observed for the film with 2 at% Mg doping concentration clearly supports the fact that Mg^{2+} ions induced into the lattice are placed in the grain boundaries or at the film surface as discussed earlier in XRD analysis. Mg^{2+} ions placed in the grain boundaries acting as recombination centers, which reduce its carrier concentration and hence resulting in an increase of its resistivity. The increased resistivity might also be due to its non-stoichiometric nature as evident from the elemental analysis (Section 3.3). The minimum values of resistivity observed for the films coated with Mg concentrations greater than 2 at% strongly favors the fact that Mg^{2+} ions got well dissolved in the CdO lattice replacing Cd^{2+} ions substitutionally which increases its carrier concentration due to increased oxygen vacancies which agrees with the compositional analysis.

3.6. PL studies

Photoluminescence (PL) is an important tool to investigate the quality of a thin film which depends on the size of the crystallites, morphology and chemical environment [26]. The PL spectra of undoped CdO and CdO:Mg thin films (Mg doping levels: 6 and 8 at%) which have better structural, morphological, optical and electrical properties, excited at $\lambda = 335$ nm are shown in Fig. 6. It was observed that the PL spectra consist of emission peaks centered at 447 nm, 495 nm, 520 nm and 546 nm respectively for both undoped and doped samples. This confirms the perfect stoichiometric nature of the doped samples. The peak centered at 447 nm may be attributed to the combination of the electrons from the conduction band and holes from the valence band. The peak at 495 nm is attributed to the excitonic transition which is size-dependent. The peak at 520 nm may be ascribed to the deep trap emission and surface state emission that is less size-dependent. This peak confirms the quantum confinement effect of the as deposited samples which is ascribed to the near-band-edge (NBE) emission of CdO [38]. This NBE emission is attributed to oxygen vacancies (V_o) and cadmium interstitials (Cd_i). This is in accordance with Acharya et al. [39] for Cd-doped ZnO thin films prepared by spray pyrolysis technique.

4. Conclusion

Mg-doped CdO films with high transparency were prepared by the spray technique using perfume atomizer. The effect of Mg doping on the structural, morphological, optical and electrical properties of the films was investigated. The films crystallizes well in cubic structure with a preferential orientation along the (1 1 1) plane irrespective of the Mg doping level. CdO thin films showed considerable variation in microstructure with Mg doping concentration. The cauliflower shaped nanostructures observed for the doped films confirmed the improvement in their crystallinity. Film transparency improves with higher Mg concentrations. Except for the film coated with 2 at% Mg, the optical band gap for the other doped samples exhibited a blue shift which was related to Burstein–Moss effect. The resistivity of the films decreases with increase in Mg concentration, and the film coated with 8 at% Mg doping exhibited a minimum resistivity of 0.0853×10^1 Ω-cm. The high optical transparency and low resistivity values obtained for the CdO:Mg films make them suitable in optoelectronic applications especially as window layer for solar cells.

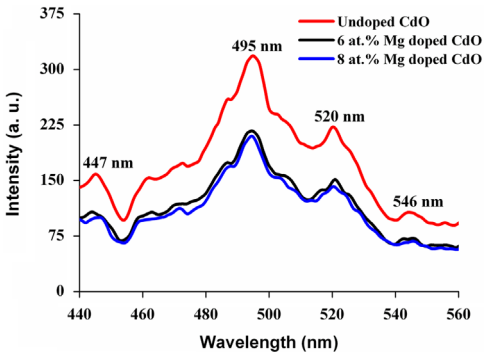

Fig. 6. PL spectra of undoped and doped CdO films with 6 and 8 at% Mg concentrations.

Acknowledgements

The authors are thankful to the Head, Department of Physics, Mr. Karthik, Alagappa University, Karaikudi for the XRD analysis, Head, Department of Chemistry and Mr. Gowtham, Gandhigram Rural Institute, Dindugal for the SEM and EDAX measurements.

References

[1] D.S. Ginley, C. Bright, Mater. Res. Bull. 25 (2000) 15–17.
[2] B.J. Lowis, D.C. Paine, Mater. Res. Bull. 25 (2000) 22–27.
[3] Z. Zhao, D.L. Morel, C.S. Ferekides, Thin Solid Films 413 (2012) 203–211.
[4] B. Saha, R. Thapa, K.K. Chattopadhyay, Solid State Commun. 145 (2008) 33–37.
[5] C.H. Champness, Z. Xu, Appl. Surf. Sci. 123 (1998) 485–489.
[6] M. Ali Yildirim, Aytune Ates, Sens. Actuators A 155 (2009) 272–277.
[7] A.R. Balu, V.S. Nagarethinam, M. Suganya, N. Arunkumar, J. Electron. Dev. 12 (2012) 739–749.
[8] B. Saha, S. Das, K.K. Chattopadhyay, Sol. Energy Mater. Sol. Cells 91 (2007) 1692–1697.
[9] R.J. Deokate, S.M. Pawar, A.V. Moholkar, V.S. Sawant, C.A. Pawar, C.H. Bhosale, K.Y. Rajpure, Appl. Surf. Sci. 254 (2008) 2187–2195.
[10] L.R. de Leon-Gutierrez, J.J. Cayente-Remero, J.M. Peza-Tapia, E. Barrera-Calva, J.C. Martinez-Flores, M. Ortega-Lopez, Mater. Lett. 60 (2006) 3866–3870.
[11] M. Bonhaliliba, C.E. Benouis, A. Tiburcio-Silver, F. Yakuphanoglu, A. Avila-Garciad, A. Tavira, R.R. Trujillo, Z. Mouffak, J. Lumin. 132 (2012) 2653–2658.
[12] K. Usharani, A.R. Balu, Acta Metall. Sin. (Eng. Lett.) 28 (2015) 64–71.
[13] L.L. Pan, G.Y. Li, J.S. Lian, Appl. Surf. Sci. 274 (2013) 365–370.
[14] F. Yakuphanoglu, Solar Energy 85 (2011) 2704–2709.
[15] M.A. Flores-Mendoza, R. Castanedo-Perez, G. Torres-Delgado, P. Rodriguez-Fragoso, J.G. Mondoza-Alvarez, J, Luminescence 135 (2013) 133–138.
[16] R.K. Gupta, K. Ghosh, R. Patel, S.R. Mishra, P.K. Kahol, Appl. Surf. Sci. 255 (2009) 4466–4469.
[17] K. Usharani, A.R. Balu, G. Shanmugavel, M. Suganya, V.S. Nagarethinam, Int. J. Sci. Res. Rev. 2 (2013) 53–68.
[18] Tokeer Ahmad, Sarvari Khatoon, Kelsey Coolahan, Samuel E. Lofland, J. Alloys Compds 558 (2013) 117–124.
[19] M. Vigneshwaran, R. Chandiramouli, B.G. Jeyaprakash, D. Balamurugan, J. Appl. Sci. 12 (2012) 1754–1757.
[20] T.D. Dzhafarov, S.S. Yesilkaya, N. Yilmaz, M. Caliskan, Sol. Energy Mater. Sol. Cells 85 (2005) 371.
[21] G.B. Abdullaev, T.D. Dzhafarov,, New York: Harwood Academic Publishers; 1987.
[22] B. Benhaoua, A. Rahel, S. Benramache, Superlattices Microstruct 68 (2014) 38–47.
[23] N. Manjula, A.R. Balu, Int. J. Chem. Phys. Sci. 3 (2014) 55–62.
[24] B.J. Zheng, J.S. Lian, L. Zhao, Q. Jiang, Vacuum 85 (2011) 861–865.
[25] A.R. Balu, V.S. Nagarethinam, A. Thayumanavan, K.R. Murali, C. Sanjeevaraja, M. Jeyachandran, J. Alloys Compds. 502 (2010) 434–438.
[26] W. Dong, C. Zhu, Opt. Mater. 22 (2003) 227–233.
[27] Q. Chang, C. Chang, X. Zhang, H. Ye, G. Shi, W. Zhang, Y. Wang, X. Xin, Y. Song, Opt. Commun. 274 (2007) 201–205.
[28] X. Liu, C. Li, S. Han, J. Han., C. Zhou, Appl. Phys. Lett. 82 (2003) 1950–1952.
[29] A. Tadjarodi, M. Imani, Mater. Lett. 65 (2011) 1025–1027.
[30] A. Tadjarodi, M. Imani, H. Kerdari, J. Nanostruct. Chem. 3 (2013) 1–8.
[31] X. Wu, T.J. Coutts, W.P. Mulligan, J. Vac. Sci. Technol. A 15 (1997) 1057–1062.
[32] J.C. Manifacier, M. DeMurcia, J.P. Fillard, E. Vicario, Thin Solid Films 41 (1977) 127–135.
[33] C. Rajashree, A.R. Balu, V.S. Nagarethinam, Int. J. Chem. Tech. Res. 6 (2014) 347–360.
[34] D.W. Ma, Z.Z. Ye, H.M. Lu, J.Y. Huang, B.H. Zhao, L.P. Zhu, H.J. Zhang, P.M. He, Thin Solid Films 461 (2004) 250–255.
[35] Y.X. Wang, X. Ding, Y. Cheng, Y.J. Zhang, L.I. Yang, H.L.L.I.H. G. Fan, Y. Liu, J.H. Yang, Cryst. Res. Technol. 44 (2009) 517–522.
[36] M. Green, Z. Hussain, J. Appl. Phys. 69 (1991) 7788–7796.
[37] G. Shanmugavel, A.R. Balu, V.S. Nagarethinam, Int. J. Chem. Mater. Res. 2 (2014) 88–101.
[38] T. Jun Kuo, Z. Micheal, H. Huang, J. Phys. Chem B110 (2006) 13717–13721.
[39] A.D. Acharya, S. Moghe, R. Panda, S.B. Shrivastava, M. Gangrade, T. Shripathi, D.M. Phase, V. Ganesan, Thin Solid Films 525 (2012) 49–55.